Journal of Engineering Science and Technology Review 16 (1) (2023) 92 - 100

Research Article

JOURNAL OF
Engineering Science and Technology Review

www.jestr.org

Preparation and Performance Analysis of Epoxy Acrylic Resin for Repairing Asphalt Pavement Diseases

Hongjun Jing[1,2,*], Xiao Mu[1,2], Qianqian Wang[3], Yuanquan Cui[1] and Changfeng Sun[4]

[1]*College of Architecture and Civil Engineering, Xi'an University of Science and Technology, Xi'an 710054, China*
[2]*Road Engineering Research Center, Xi'an University of Science and Technology, Xi'an 710054, China*
[3]*Shaanxi Provincial Highway Bureau, Xi'an 710068, China*
[4]*YuLin Highway Bureau, Yulin 719000, China*

Received 25 February 2022; Accepted 19 March 2023

Abstract

Considering the poor cohesiveness of the joint between pothole repair materials on asphalt pavement and old pavement, epoxy resin (EP) was toughened in this study, and a new composite resin material applicable to pavement repair was proposed. In particular, epoxy acrylic resin was prepared through the blending modification of acrylic resin and EP. The rheological properties of the composite resin were analyzed, and the influence of different acrylic acid contents on the toughness of the composite resin was discussed. Subsequently, the curing reaction process of the composite resin was explored via differential scanning calorimetry, and the theoretical curing process was determined. On this basis, the thermal stability of the composite resin was analyzed through thermogravimetric analysis. Results show that the tensile strength, elongation at break, and impact strength of the optimal composite resin are increased by 88.43%, 4202%, and 103.14%, respectively compared with those of EP alone, indicating that acrylic resin exerts a remarkable toughening effect on EP. The construction process parameters of the resin can be effectively predicted by measuring the curing reaction degree. The onset temperature of the resin is 101 ℃, and its thermal stability is favorable and can meet the application requirements of the resin in high-temperature weather during summer. The conclusions provide an important reference for follow-up research on pavement maintenance materials.

Keywords: Asphalt pavement, Epoxy acrylic resin, Mechanical properties, Curing reaction, Thermal stability

---

1. Introduction

Asphalt pavement, a flexible pavement structure composed of asphalt mixture, various base layers, and cushion layers, has become the primary pavement form at present because it exhibits good smoothness, offers convenient construction and maintenance, and ensures comfortable driving. With the rapid development of China's traffic industry, road traffic volume has surged and the vehicle load borne by asphalt pavements has been increasing along with loading frequency. Under the combined effects of environmental factors and vehicle loads, cracks, pits, ruts, and other diseases have appeared on asphalt pavements before they reach their designed service life. Such diseases have seriously affected the stability, safety, and comfort of driving, and impact load caused by vehicle bumps and vibrations induced by pavement diseases is 1.5–2.0 times that of normal pavements [1]. Surface water seeps into the pavement structure layers through the diseased parts, resulting in the loosening and peeling of pavement surface materials, the softening of pavement base materials, the reduction of bearing capacity, and other phenomena. Consequently, asphalt pavements are subjected to crack expansion, local subsidence, or pothole expansion, affecting the service life of roads and triggering economic losses.

With the increasing prominence of diseases on asphalt pavements, the key problem in China's road construction lies in improving the maintenance and repair technologies of asphalt pavements. At present, most maintenance and repair methods for asphalt pavements in China address emergency maintenance and repair, which require low cost and fast construction. However, with the development of road cause, the maintenance technology for asphalt pavements in China is changing from emergency maintenance to preventive maintenance [2]. As a typical disease of asphalt pavements, potholes seriously affect smoothness and driving comfort along pavements. The service life of asphalt pavements can be effectively prolonged by repairing potholes as soon as possible. Hot-mixed asphalt mixtures are characterized by high strength, good stability, and good compatibility with old pavements when used as pothole repairing materials. However, hot-mixed asphalt pavements cannot be constructed during winter and rainy season, and potholes on asphalt pavements cannot be repaired on time, affecting road traffic [3]. Cold-mixed asphalt mixtures can be spread whenever possible and conveniently constructed without heating; moreover, they are applicable to pothole repair construction during low-temperature seasons and rainy days [4]. Investigations on the present situation of pavement pothole repair have found that cohesiveness at the joint between common pothole repair materials and pavement is poor, reducing the integrity of the original pavement. Moreover, rainwater and oil stains on the pavement permeate through the joint between old and new asphalt mixtures. After the repair, the surrounding parts of potholes tend to loosen, and the repair materials fall off. During the braking process of vehicles, the secondary damages of shearing and extrusion occur within a short time, and

---

*E-mail address: jinghongjun@xust.edu.cn

ISSN: 1791-2377 © 2023 School of Science, IHU. All rights reserved.
doi:10.25103/jestr.161.12

potholes reappear on the pavement, increasing maintenance workload and cost [5-6].

Specific to the cohesiveness problem of the joint between the pothole repair material and the original pavement, the new–old asphalt joints are slotted and then poured with the binding material [7] to enhance their cohesiveness by referring to the potting adhesives commonly used on asphalt pavements. However, construction technology is complicated, with poor economic applicability. The joint of the repaired potholes can be covered by seal bands, forming a "cap" [8], to increase the bonding force at the joint. Nevertheless, existing seal bands in China are brittle at low temperatures and lose their cohesiveness to the pavement when heated at high temperatures during summer, and thus, their service life is short. To improve the integrity of damaged asphalt pavement after repair, reduce the erosion of subgrade pavement caused by rainwater infiltration, and prolong the service life of the repaired asphalt pavement, a type of pavement resin coating with good flexibility and strong adhesion was proposed in the current study, and the thermal effect of its curing process was analyzed.

2. State of the art

As a common resin polymer material, epoxy resin (EP) reacts with curing agents to produce cross–linked products that exhibit excellent cohesiveness, good mechanical properties, and small curing shrinkage [9-11]; thus, it is widely used in the building industry, chemical coatings, road traffic, and aerospace. Its operating temperature range is wide, and the cross-linking degree of resin curing products can be controlled well by selecting the category of curing agents and controlling curing temperature. After cross-linking curing, however, single EP becomes hard and brittle in texture, poor in toughness, low in impact strength, and poor in weather resistance [12]; hence, its technical requirements cannot be met when used in asphalt pavements. Therefore, modifying and toughening EP are highly significant for solving the application problem of EP in pavement resin coatings.

At present, many scholars have exerted effort to achieve the toughening effect by modifying EP. The active groups in rubber react with epoxy macromolecules, and the mechanical properties of the modified resin are evidently improved, realizing the toughening modification of EP. Gunwant et al. [13] modified the diglycidyl ether of bisphenol A EP with liquid rubber (LR). Through the tensile test and analysis of fracture surface morphology, LR was found to improve the toughness of EP. Ratna et al. [14] mixed synthesized carboxyl-terminated polyethylhexyl acrylate LR with EP for pre-reaction and obtained modified EP. The results showed that the impact strength of the modified resin was about three times that of the unmodified EP. Li et al. [15] explored the fracture properties of polysulfide rubber and polyaniline-modified EP. The results revealed that the toughening effect of the three materials was remarkable under the optimal blending ratio, and the materials were transformed from brittle fracture to ductile fracture. Nano-fillers exhibit a large specific surface area, strong interfacial action, and high hardness. When introduced, EP endows the resin system with many advantages of inorganic nano-fillers and achieves the purpose of toughening EP. Ghosh et al. [16] considered the agglomeration of nanoparticles. Nano-TiO_2 was dispersed in the EP matrix by an ultrasonic dispersion method, and the toughness of the resin reached the maximum when the dosage of nano-TiO_2 was 10%. The adhesive strength and fracture toughness of EP that contained cellulose nanocrystals (CNC) prepared by Pruksawan et al. [17] were considerably improved. Its tensile shear strength reached 29 MPa and its fracture toughness reached 389 $MPa \cdot m^{1/2}$, which were 125% and 378%, respectively, higher than those of EP without CNC. Saadati et al. [18] modified and toughened EP by cross-linking ethenyl and hydroxyl-terminated polybutadiene. The results indicated that when the mass ratio of ethenyl to hydroxyl-terminated polybutadiene was 20:100, the material acquired the best impact and mechanical properties. Kong et al. [19] used toluene diisocyanate and polypropylene glycol to synthesize isocyanate-terminated polyether and synthesized EP with flexible segments by using the reaction of isocyanate-terminated polyether with EP, which not only improved the curing flexibility of EP but also increased its adhesion. In the preceding research, rubber, as a modified material, cannot realize phase separation during the curing reaction of the EP system, easily decreasing the glass transition temperature of the resin and affecting its thermal stability at high temperatures. Interaction between nanoparticles is strong, and the dispersion problem in resin modification is still not solved well. Synthesizing block copolymers is difficult, and impurities can be easily introduced. All the above materials have some adverse effects on modified EP.

After toughening modification, the curing reaction conditions of the resin exert considerable influence on film-forming performance. Therefore, the curing reaction process of the resin should be tracked and controlled during the preparation of epoxy acrylic resin. Infrared spectroscopy can directly reflect the chemical structure changes of the resin during the curing reaction, and the kinetic parameters in the curing reaction of the resin matrix can be determined by observing the change rules of active groups during the curing reaction of the resin [20-21]. Vashurkin et al. [22] divided the vertical peak of the spectrum into a single peak in the near-infrared range and calculated the concentration of the functional groups of the resin. The conversion rate of the epoxy groups in the resin reached the maximum value at 140 °C. Weiss et al. [23] studied the isothermal curing degree of melamine resin at different temperatures via online infrared spectroscopy. Despite its rapidness and convenience, this method can only identify the functional groups of the cured resin and cannot track the curing process of the resin. In addition, the measurement process is easily interfered with by other functional groups with similar peak values, affecting the accuracy of the measurement results.

In consideration of the shortcomings of existing research, BS-104-2 acrylic resin (BS) with high molecular weight, good toughening effect, and weather resistance was selected in the current study to perform toughening modification of EP, aiming to synthesize composite resin–epoxy acrylic resin (EAM) and prepare a type of resin coating material with favorable toughness and hardness. On this basis, the curing process and thermal stability of the curing products of the composite resin prepared through the best formula were analyzed via differential scanning calorimetry (DSC) and thermogravimetric analysis (TG), and the applicability of the coating to construction was predicted.

The remainder of this study is organized as follows. In Section III, the material preparation process and test method are expounded. In Section IV, the test results of the composite resin, including its viscosity, mechanical properties, and thermal properties, are analyzed. Then, a curing kinetic model is established. In the final section, the study is summarized and relevant conclusions are drawn.

3. Methodology

3.1 Test profile

3.1.1 Raw materials

EP: bisphenol A-type EP E-51, Sinopharm Chemical Reagents Co., Ltd.; acrylic resin: BS-104-2, Sanmu Group Chemical Reagent Co., Ltd.; curing agent: 593 curing agent, Sinopharm Chemical Reagent Co., Ltd.; accelerator: DMP-30, Sinopharm Chemical Reagents Co., Ltd.; defoamer: SH-5500, Foshan Lixin Chemical Co., Ltd.

3.1.2 Sample preparation

In accordance with Table1 formulation, EP and BS were weighed and poured into a beaker. The mixture was stirred with a glass rod at room temperature. After the two resins were fully blended, other auxiliaries, such as the curing agent, were quantitatively added to the edge of the beaker step by step, following a certain order. Then, the mixture was fully stirred using a glass rod and set aside for later use. The detailed resin preparation process is illustrated in Fig. 1.

Table 1. Formula for the composite resin

Sample name	E-51:BS-104-2
EAM0	100:0
EAM1	100:10
EAM2	100:20
EAM3	100:30
EAM4	100:40
EAM5	100:50

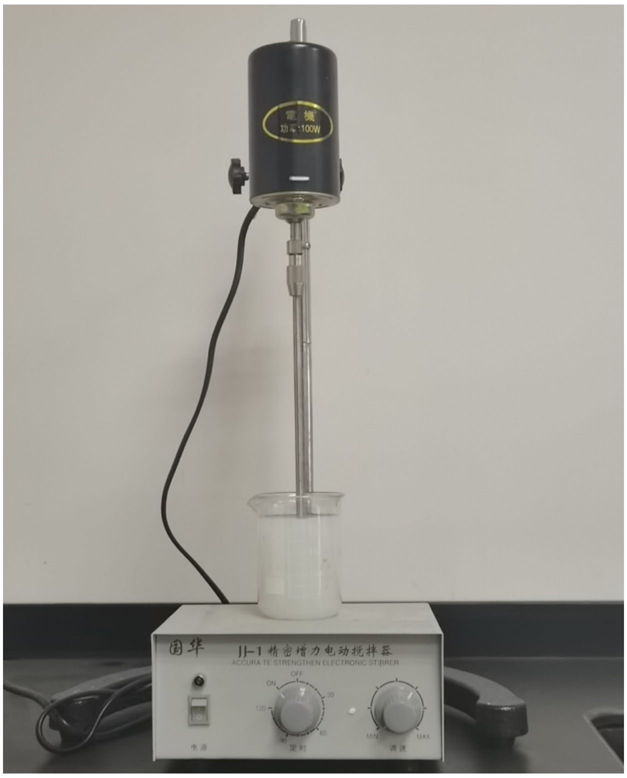

Fig. 1. Preparation process of epoxy acrylic resin

3.2 Test method

3.2.1 Viscosity test

A Brinell viscometer (NDJ-1D) (Fig. 2) was used to determine the temperature-dependent variation trend of the viscosity of the mixed composite resin at a heating rate of 3 ℃/min within a test temperature range of 20 ℃–80 ℃.

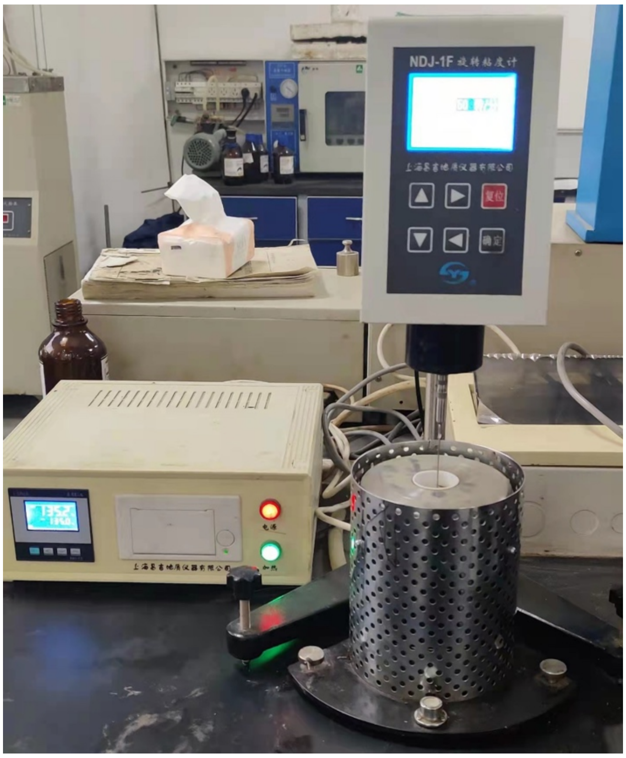

Fig. 2. NDJ-1D Brookfield viscometer

3.2.2 Tensile strength and elongation at break test

A universal testing machine (CMT5105) (Fig. 3) was employed to test the tensile strength and elongation at break of specimens at a stretching rate of 10 mm/min in accordance with GB/T2567-2021.

Fig. 3. CMT5105 universal testing machine

3.2.3 Impact strength test

A simply supported beam impact tester (XCJD-50) was used to test the impact toughness of the specimens at an impact speed of 2.9 m/s in accordance with GB/T2567-2021.

3.2.4 Shore hardness test

A Shore hardness tester (LX-D type) was utilized to test the hardness of the specimens. Three groups of data were tested for each specimen, and the average value was considered.

3.2.5 Non-isothermal DSC test

A differential scanning calorimeter (200 F3) was employed to track the curing reaction process of the resin, and high-purity indium was used for temperature correction. Then, 5 mg of the EP–acrylic acid system specimen was weighed and placed in an aluminum crucible in high-purity nitrogen atmosphere. After bottom sealing, the specimen was scanned by heating from 30 °C to 250 °C at different heating rates (5, 10, 15, and 20 K/min).

3.2.6 TG test

A TG analyzer (TG209 F3) was used to analyze the temperature–mass loss of the cured resin. Here, 2.5 mg of the specimen was placed in a crucible under nitrogen atmosphere, with a heating rate of 5 K/min and a scanning range of 0 °C–500 °C.

4. Result analysis and Discussion

4.1 Performance characterization of EAM

4.1.1 Rheological properties of EAM

The viscosity of EP, a thermosetting resin, changes with the cross–linking reaction during curing. BS, which has low viscosity, can dilute EP and prolong the applicable time of resin during curing construction. Fig. 4 depicts the viscosity–temperature curves of EAM at different mixing proportions. As shown in the figure, EAM was a viscous liquid at room temperature, and its initial viscosity decreased with the addition of BS. At 20 °C–43 °C, the groups in the system gain energy with an increase in system temperature, reaction activity was strengthened, and system viscosity decreased considerably. At 43 °C–68 °C, the fluctuation range of EAM viscosity was about 200 mPa·s. When temperature was higher than 68 °C, the cross-linking degree of EAM increased more than the activity of the molecular chain movement caused by the temperature rise, and the system entered a gel state, with its viscosity starting to rise sharply. The viscosity of EAM5 remained stable after dropping to 200 mPa·s, proving that EAM5 had not experienced curing reaction. EAM had a wide temperature range in the transformation process from a liquid state to a gel state. This condition was beneficial for the actual operation and construction of resin materials.

4.1.2 Mechanical properties of EAM

After curing, EP exhibits poor toughness and is prone to brittle failure, leading to the failure of the overall coating structure. Therefore, the resin coating is required to be of certain toughness and hardness after curing. Toughness is divided into fracture toughness and impact toughness. As a property of the material itself, fracture toughness is a measure of the material's resistance to brittle failure. Impact toughness indicates the ability of a material to resist external impact. In the current study, tensile strength, elongation at break, and impact strength were used to characterize the toughness of the composite resin. In accordance with Fig. 4, four formulations (EAM1, EAM2, EAM3, and EAM4) were selected to prepare the specimens, and their tensile mechanical properties were tested after curing at room temperature, with EAM0 as the blank control group.

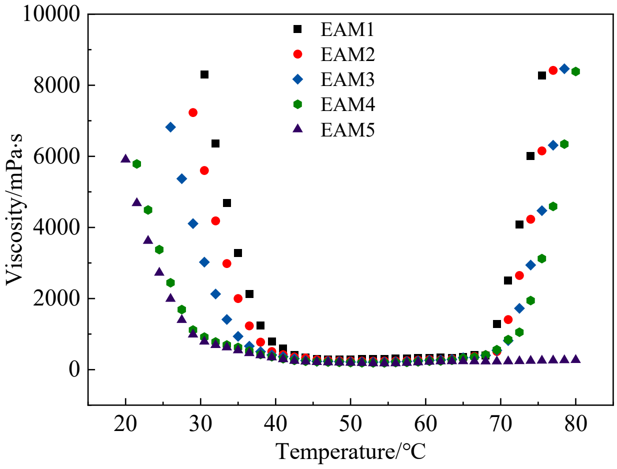

Fig. 4. Viscosity–temperature curves of EAM

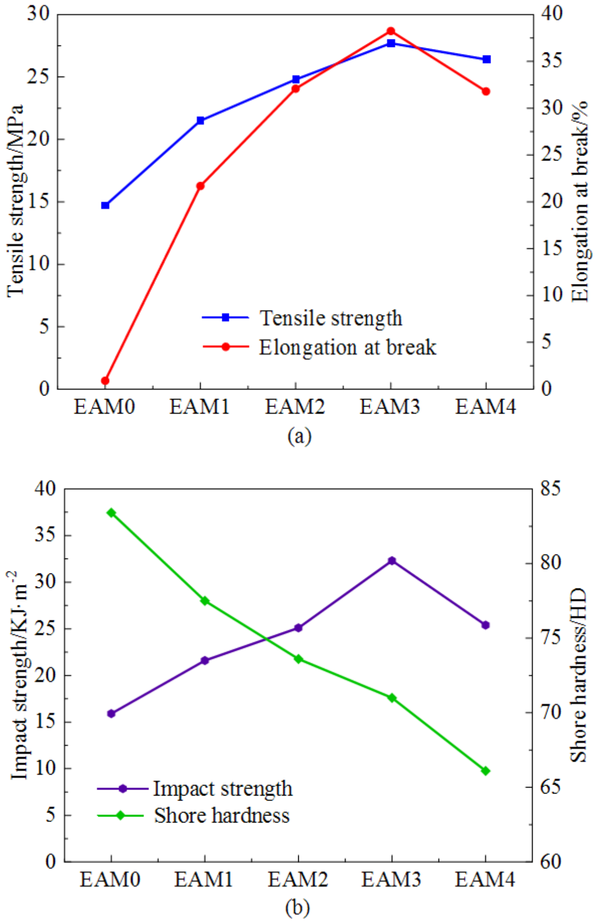

Fig. 5. Mechanical property test of EAM (a)Tensile strength and elongation at break (b)Impact strength and Shore hardness

Fig. 5(a) depicts the variation trends of the tensile strength and elongation at break of EAM at different dosage levels. With an increase in BS content, the tensile strength and elongation at break of EAM initially increased and then decreased. When the optimal BS content was 30 portions, the tensile strength is 88.43% higher than that of EAM0 (pure EP). The elongation at break of the specimen initially increased and then decreased with an increase in BS content, and the change curve is shown in Fig. 5(a). When 30 portions of BS were used, the elongation at break of the EAM3 specimen was 37.8%, which was the maximum value. When the amount of BS was increased to 40 portions, the tensile strength of the material decreased, physical entanglement played a role in the tensile strength of the material, and elongation at break began to decrease.

Fig. 5(b) presents a broken line chart of the numerical changes in the impact strength and Shore hardness of EAM at different mixing proportions. By adding the BS modifying material to the EP matrix, the impact strength of EAM gradually increased with an increase in BS content. When 30 portions of BS were added, the impact strength of EAM3 was 103.14% higher than that of pure EP, while the impact strength of resin decreased when BS was continuously added.

When the driving load is directly in contact with the asphalt pavement surface, it will induce obvious cracks on the pavement and form stress concentration. Therefore, a certain toughness requirement was proposed in the current study for the prepared pothole repair coating material of the asphalt pavement, expecting to relieve the plastic deformation brought by vehicle loads. When 30 portions of BS were added, the tensile strength of EAM3 was 27.7 MPa and the elongation at break was 38.24%, which were 88.43% and 4202% higher than those of EAM0, respectively. The fracture toughness of the resin was the best. Simultaneously, the impact strength of EAM3 increased by 103.14% to the highest value of 32.3 KJ/m^2 within a suitable hardness range. Its impact toughness was also considerably improved. In summary, the resin had the best toughness and certain hardness in this case, and thus, it has good practicability as pavement coating.

4.2 Reaction heat and characteristic temperature of EAM3

4.2.1 Non-isothermal DSC analysis of EAM3

Fig.6 displays the heat flow–temperature spectrum of EAM3 at heating rates of 5, 10, 15, and 20 K/min. As shown in Fig. 6, EAM3 only had a single exothermic peak of curing reaction at different heating rates, indicating a single curing mechanism in the system, without evident side reactions. With an increase in heating rate, the heat release per unit time increased and relative curing time was shortened. The reaction heat release of the resin system lagged behind, and the initial temperature and exothermic peak of curing reaction moved toward high temperatures.

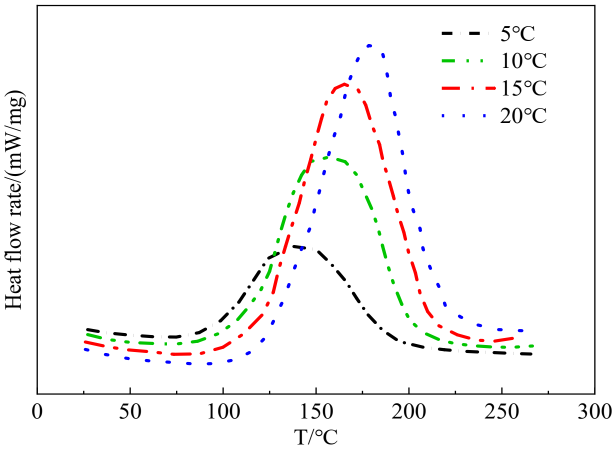

Fig. 6. DSC curves of EAM3 at different heating rates

4.2.2 Changes in the conversion rate of EAM3

By integrating the exothermic peaks of the curing reaction of EAM3 at different heating rates, the relation curves between EAM3 conversion rate and curing temperature can be obtained, as shown in Fig. 7.

The resin conversion curve shifted to high temperatures with an increase in heating rate. During the initial reaction stage, when $\alpha \leq 20\%$, the heat could not be transferred inward from the surface of EAM3, a few active groups were present in the resin, and conversion rate increased slowly. During the rapid development stage of the reaction, when $20\% \leq \alpha \leq 80\%$, viscosity decreased, heat was transferred inward from the surface of EAM3, active groups increased considerably, curing reaction rate increased sharply, and conversion rate increased rapidly. During the completion stage, when $\alpha \geq 80\%$, the cross-linking density and viscosity of EAM3 gradually increased, the movement of its internal active groups was blocked, and conversion rate increased slowly. The synthesized EAM3 had a certain heat capacity and a low thermal conductivity coefficient, and thus, it was affected by the thermal lag effect of the system. When heating rate was accelerated, the temperature of the system would not change immediately. At this moment, the conversion rate–temperature curve moved rightward (high temperature).

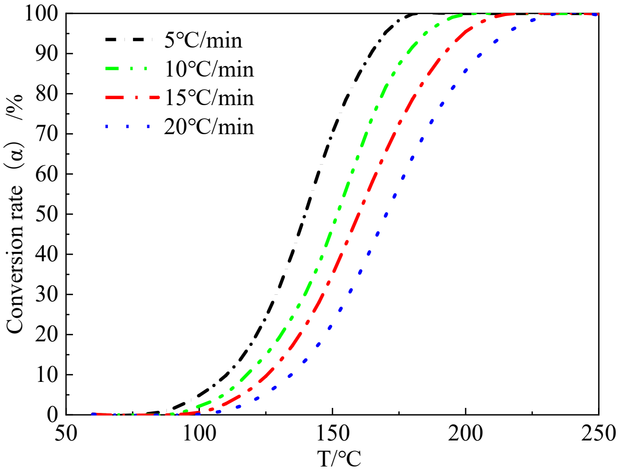

Fig. 7. EAM3 conversion rate–temperature relation curves

The resin conversion curve shifted to high temperatures with an increase in heating rate. During the initial reaction stage, when $\alpha \leq 20\%$, the heat could not be transferred inward from the surface of EAM3, a few active groups were present in the resin, and conversion rate increased slowly. During the rapid development stage of the reaction, when $20\% \leq \alpha \leq 80\%$, viscosity decreased, heat was transferred inward from the surface of EAM3, active groups increased considerably, curing reaction rate increased sharply, and conversion rate increased rapidly. During the completion stage, when $\alpha \geq 80\%$, the cross-linking density and viscosity of EAM3 gradually increased, the movement of its internal active groups was blocked, and conversion rate increased slowly. The synthesized EAM3 had a certain heat capacity and a low thermal conductivity coefficient, and thus, it was affected by the thermal lag effect of the system. When heating rate was accelerated, the temperature of the system would not change immediately. At this moment, the conversion rate–temperature curve moved rightward (high temperature).

Table 2. Non-isothermal kinetic characteristic parameters of EAM3

β/(K/min)	T_i/°C	T_p/°C	T_f/°C
5	87.3	145.2	186.3
10	95.3	157.2	205.6
15	103.9	164.7	221.1
20	108.0	175.2	238.3

In the table, β is the heating rate, K/min; T_i denotes the initial temperature, °C; T_p is the peak temperature, °C; and T_f represents the termination temperature, °C.

4.2.3 Characteristic temperature analysis of EAM3

The curing reaction temperature of the system is considerably affected by heating rate, and when the resin is actually used, it is generally at a constant temperature. To eliminate the influence of the change in heating rate on reaction heat, the T_i, T_p, and T_f at different heating rates in Table 2 were plotted in Fig. 8 and linearly fitted. The approximate gel temperature (T_{i0}), curing temperature (T_{p0}), and after-treatment temperature (T_{f0}) at β=0 K/min were obtained via T–β extrapolation, and they were 80.95 °C, 136.20 °C, and 169.95 °C, respectively.

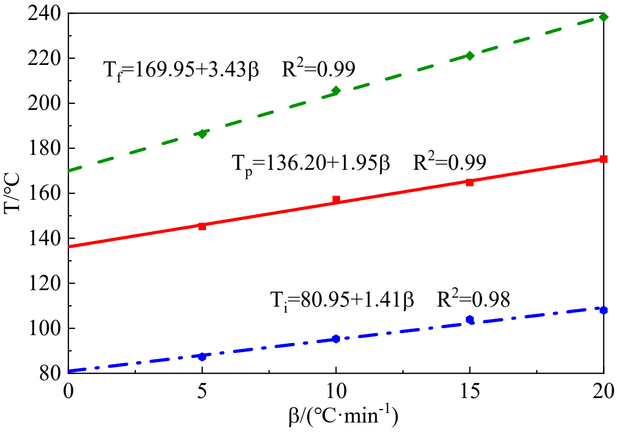

Fig. 8. Extrapolated straight line obtained through the linear fitting of T–β

T_{p0} and T_{f0} were acquired through the extrapolated straight line in Fig. 8. Considering the internal heat accumulation in the resin during practical applications, the actual curing temperature of EAM3 is slightly lower than 136.20 °C. In the current study, 130 °C was selected as the curing temperature and 150 °C as the post-curing temperature. In the actual curing reaction, the thermal conductivity of the resin system is low, accompanied by an excessively fast heating rate and an uneven temperature field of the system, resulting in the uneven shrinkage of EAM during the curing process and further leading to internal stress and material deformation. Moreover, debonding and cracking may occur, affecting the service life of the material. In the current study, the curing method of 130 °C/ 100 min+150 °C/ 30 min was adopted. After EAM3 was cured at 130 °C for 100 min, temperature was raised to 150 °C and curing time was prolonged for 30 min, reducing internal stress during curing and facilitating the system to achieve the best curing performance. The theoretical calculation value provides an important basis for determining the actual curing process parameters of EAM3.

4.3 Curing kinetic model of EAM3

The thermal activation reaction was analyzed and predicted to deduce the reaction process suitable for various heat treatment methods (including linear heating and other non-isothermal treatment methods) for a comprehensive description. On the basis of the different temperature dependence of the thermal activation reaction, the conversion rate in the reaction process was simplified, and the reaction rate can be expressed by the following formula:

$$\frac{d\alpha}{dT}=\frac{1}{\beta}k(T)f(\alpha) \tag{1}$$

where E represents the reaction activation energy, KJ/mol; and A denotes the pre-exponential factor, min^{-1}.

4.3.1 Kissinger method

As assumed by the Kissinger method [24], the reaction temperature is the highest at the peak of the thermal analysis curve, which is unaffected by heating rate, with its n-order reaction model as follows:

$$ln\left(\frac{\beta}{T_p^2}\right)=ln\frac{AR}{E}-\frac{E}{RT_p} \tag{2}$$

where R is the molar gas constant, being 0.00831 KJ/(mol·K).

The $ln(\beta/T_p^2)$–$1/T_p$ relation curve was drawn in accordance with Table 2 and linearly fitted. As shown in Fig. 9(a), E was solved as 66.15 KJ/mol on the basis of the straight slope and A as 4.46×10^7 on the basis of the intercept.

The reaction order n was determined through the Crane method [25], as presented in Eq. (3).

$$\frac{d(ln\beta)}{d\left(\frac{1}{T_p}\right)}=-\left(\frac{E}{nR}+2T_p\right) \tag{3}$$

The $ln\beta$–$1/T_p$ relation curve was plotted and linearly fitted, as shown in Fig 9(b), where E=66.15 KJ/mol was substituted to obtain the reaction order n as 0.90.

The obtained parameters were substituted into the n-order reaction kinetic model for integral transformation to obtain the relational expression among α, t, and T [Eq. (4)]:

$$\alpha(t)=1-\left(1-4.46\times10^6 e^{-\frac{66150}{8.31T}}t\right)^{10} \tag{4}$$

where α is the conversion rate, %; t represents the curing time, min; and T denotes the curing temperature, K.

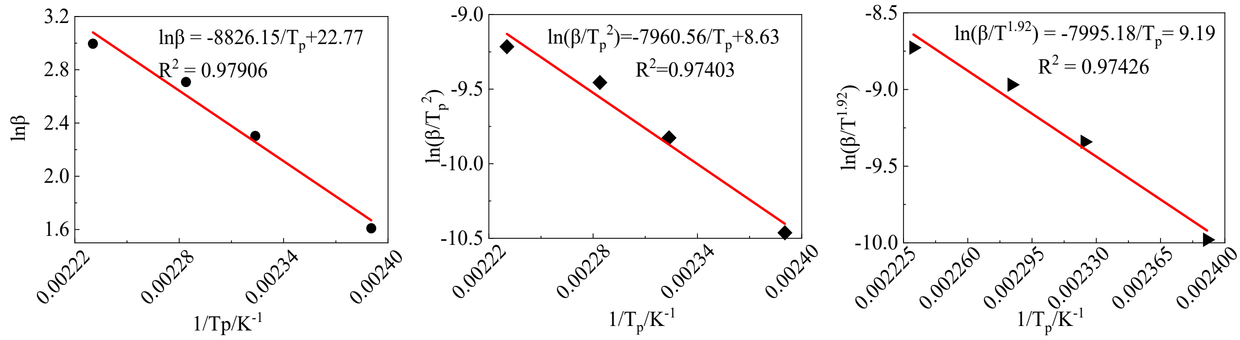

(a) (b) (c)

Fig. 9. Relation curve chart. (a) $ln(\beta/T_p^2)–1/T_p$ (b) $ln\beta–1/T_p$ (c)$ln(\beta/T^{1.92})$ $–1/T$

As revealed by the relational expression, i.e., Eq. (4), conversion rate grew with an elevation of curing temperature and the lengthening of curing time. The curing temperature of 403.15 K, i.e., 130 °C, was substituted into Eq. (4) to obtain the conversion rate of the system as 99.9% at 100 min.

4.3.2 Starink method

The Starink equation [26] acquires the activation energy by using a multiple scanning rate and an equivalent conversion rate, and its general formula under non-isothermal conditions is

$$ln\left(\frac{\beta}{T^{1.92}}\right)=Const-1.0008\frac{E}{RT} \tag{5}$$

Table 3. Curing reaction kinetic parameters of EAM3

Kissinger equation		Starink equation	$E_{ave/}$ (KJ/mol)	Crane equation
E/(KJ/mol)	A/min⁻¹	E/(KJ/mol)		n
66.15	4.46×10^7	66.39	66.27	0.90

Note: E_{ave} is the average value of the solved activation energy.

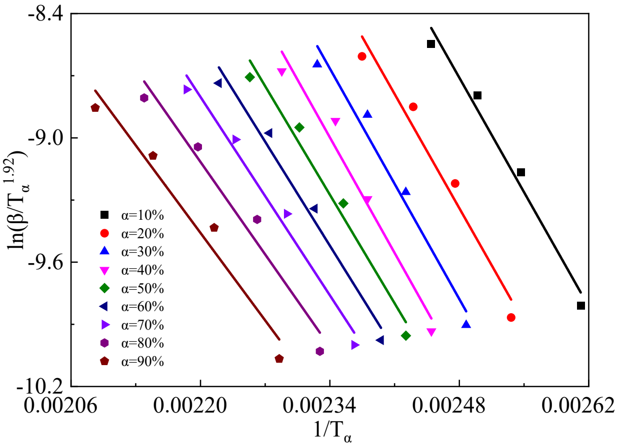

Fig. 10. $ln(\beta/T_\alpha^{1.92})–1/T_\alpha$ relation curve chart of EAM3

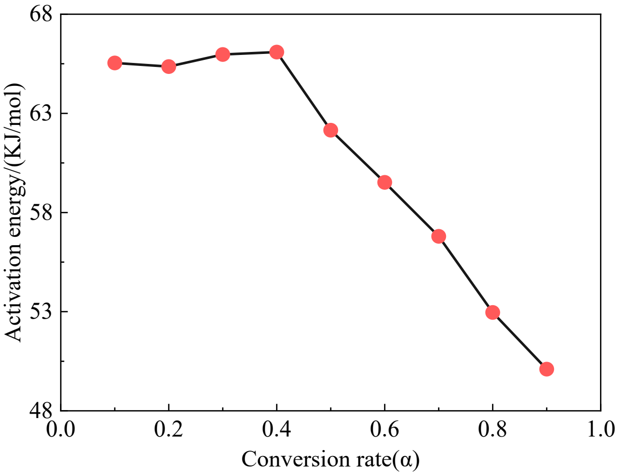

Fig. 11. $E–\alpha$ relation curve chart

The $ln(\beta/T^{1.92})–1/T$ relation curve chart of EAM3 was plotted, as shown in Fig. 9(c). The system activation energy E at its peak temperature can be solved as 66.39 KJ/mol in accordance with the slope of the fitted curve, namely, $−1.0008$ E/R. The curing reaction kinetic parameters of EAM3 are shown in Table 3.

The linear fitting line of $ln(\beta/T_\alpha^{1.92})–1/T_\alpha$ at different conversion rates is shown in Fig.10. In accordance with the calculation results, the activation energy E line chart at different conversion rates could be drawn, as shown in Fig.11. As the conversion rate of EAM3 increased, the broken line exhibited a trend of gentle increase at first and then a rapid decrease. When $\alpha\leq0.4$, the energy absorption rate of EAM3 was slow due to its own thermal lag effect, and the activation energy value was stabilized within 65–66 KJ/mol. In this case, the activation energy was large and the trend was gentle. With an increase in conversion rate, the curing degree of EAM3 increased, viscosity increased rapidly, diffusion control started playing a dominant role in the reaction, and activation energy presented an evident declining trend.

4.4 Thermal stability analysis of EAM3

The resistance of polymers to thermal deformation and thermal decomposition is the thermal stability of a material. In this experiment, TG analysis was used to characterize the thermal stability of EAM3 curing products by measuring the relationship between the material mass and temperature. Considering the thermal hysteresis of the curing product itself, the temperature increase rate of 5 K/min was used for the test. Fig. 12 shows the TG curve chart of the curing product in nitrogen atmosphere.

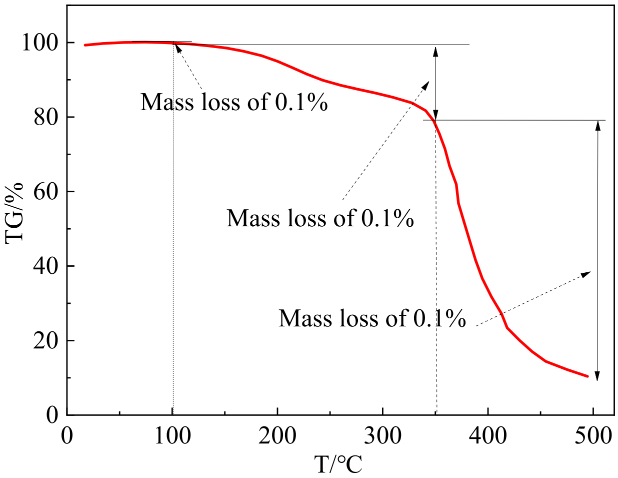

Fig. 12. TG curve chart of EAM3 curing products

The thermal weight loss of EAM3 curing products can be divided into three stages. At temperatures of 0 °C–101 °C, the weight loss rate of the sample was the lowest, and the curing product was glassy and exhibited good thermal stability. At 101 °C–353.9 °C, the weight loss curve of the sample was gentle, and evident mass loss started. When temperature exceeded 101 °C, the resin material transited to a highly elastic state. At this moment, the residual solvent in the curing product was volatilized, network structure was destroyed slightly, and mass loss was small. As temperature continued to rise, most organic compounds started oxidative decomposition at 200 °C–300 °C, and weight loss increased, affecting thermal stability. The front segment of the weight loss curve was gentle, with a sudden change at 353.9 °C. Under this circumstance, the sample underwent thermal degradation and began to change from a highly elastic state to a viscous flow state. At 353.9 °C–500 °C, the mass loss percentage of the sample reached 72.91%, and the mechanical properties of the material were completely lost at this stage. The measured glass transition temperature of the curing product was considerably higher than the service temperature of the composite resin, indicating its good thermal stability in practical applications.

5. Conclusion

To prolong the service life of asphalt pavement disease repair materials and considering the shortcomings of the existing pavement repair materials, EAM was synthesized by BS-modified EP to prepare a composite resin for pavement disease repair. Then, the suitable composite resin formulations EAM0, EAM1, EAM2, EAM3 and EAM4 were obtained according to the viscosion-temperature curve test results of resin materials in different proportions. Finally, the following conclusions were drawn through the performance test.

(1) EAM3 was considered a formula with the best toughness by testing the tensile strength, elongation at break, impact strength grade, and Shore hardness of the five types of composite resins.

(2) The characteristic temperature of EAM3 was obtained on the basis of non-isothermal DSC. Then, 130 °C/100 min+150 °C/30 min was recommended as the curing process of the resin in field construction.

(3) The average activation energy and reaction order of EAM3 were solved as 67.43 KJ/mol and 0.90, respectively, by using the Kissinger, Crane, and Starink methods. On this basis, a system reaction model was established.

(4) As revealed by TG, the mass loss of the EAM3 curing product was only 0.1% within a temperature range of 0 °C–101 °C.

The epoxy acrylic resin for repairing asphalt pavement diseases proposed in the current study exhibits good toughness, a simple preparation process, good thermal stability when coating materials at room temperature, and certain economic practicability. However, the test in this work remained at the indoor test and theoretical derivation stages. Further optimizing the mixing proportion and curing process of pavement coating materials through practical engineering applications is suggested.

References

1. Wu, L., “On damage types of asphalt pavement potholes and its restoration measures”. *The China Municipal Engineering*, (4), 2010, pp.11-13.
2. Wu, Y., “Present situation and countermeasures of highway maintenance technology development in China”. *Traffic World*, (4), 2003, pp.42-44.
3. Ahmed, T. M., Al-Khalid, H., Ahmed, T. Y., “Review of techniques, approaches and criteria of Hot-Mix asphalt fatigue”. *Journal of Materials in Civil Engineering*, 31(12), 2019, pp. 03119004.
4. Boateng, K. A., Tuffour, Y. A., Obeng-Atuah, D., Agyeman, S., “Quality of cold-mix asphalt in bituminous pavement maintenance in Ghana: Preliminary indications”. *Case Studies in Construction Materials*, 15(15), 2021, pp. e00769.
5. Chen, J., Ho, H., Liao, M., Wang, T., “Engineering properties of asphalt concrete patching mixtures”. *Journal of Testing and Evaluation*, 44(1), 2016, pp.534-542.
6. Guo, Y., Sheng, A., Zhang, J., Sun, Z., “Experimental research of tack coat materals’ performance on asphalt pavement”. *Journal of Chang 'an University (Natural Science Edition)*, 31(6), 2011, pp.16-20.
7. Wang, H., “*Development and application of high performance crack treatment material for asphalt pavement*”. Master thesis of Chongqing Jiaotong University, China, 2019, pp.18-20.
8. Li, F., Shi, X., Xu, J., “Performance evaluation and technical requirements of asphalt pavement crack seal band”. *Journal of Beijing University of Technology*, 39(12), 2013, pp.1855-1860.
9. Mousavi, S. R., Estaji, S., Javidi, M. R., Paydayesh, A., Khonakdar, H. A., Arjmand, M., Rostami, E., Jafari, S. H., “Toughening of epoxy resin systems using core–shell rubber particles: a literature review”. *Journal of Materials Science*, 56(33), 2021, pp.18345-18367.
10. Hsissou, R., “Review on epoxy polymers and its composites as a potential anticorrosive coatings for carbon steel in 3.5% NaCl solution: Computational approaches”. *Journal of Molecular Liquids*, 336(336), 2021, pp.116307.
11. Wang, T., Huang, P., Li, Y., He, N., Fu, S., “Epoxy nanocomposites significantly toughened by both poly(sulfone) and graphene oxide”. *Composites Communications*, 14(14), 2019, pp.55-60.
12. Sprenger, S., “Epoxy resins modified with elastomers and surface-modified silica nanoparticles”. *Polymer*, 54(18), 2013, pp.4790-4797.
13. Gunwant, D., Sah, P. L., Zaidi, M.G.H., “Morphology and micromechanics of liquid rubber toughened epoxies”. *e-Polymers*, 18(6), 2018, pp.511-527.

14. Ratna, D., Banthia, A.K., Deb, P.C., "Toughening of epoxy resin using acrylate-based liquid rubbers". *Journal of Applied Polymer Science*, 78(4), 2000, pp.716-723.
15. Li, X., Zhang, X., Gong, J., Zhang, L., Ye, N., Li, H., Lei, L., "Mechanical properties as well as thermal stability and anticorrosion behavior of epoxy resin/polyaniline paint toughened by polysulfide rubber". *Material Protection*, 47(7), 2014, pp.18-20+7.
16. Ghosh, P. K., Pathak, A., Goyat, M. S., Halder, S., "Influence of nanoparticle weight fraction on morphology and thermal properties of epoxy/TiO_2 nanocomposite". *Journal of Reinforced Plastics and Composites*, 31(17), 2012, pp.1180-1188.
17. Pruksawan, S., Samitsu, S., Fujii, Y., Torikai, N., Naito, M., "Toughening efect of rodike ellulose nanocrystals in epoxy adhesivel". *ACS Aplied Polymer Materials*, 2(3), 2020, pp.1234-1243.
18. Saadati, P., Baharvand, H., Rahimi, A., Morshedian, J., "Effect of modified liquid rubber on increasing toughness of epoxy resin". *Iranian Polymer Journal*, 14, 2005, pp.637-646.
19. Kong, Z., Zou, L., Zhang, Y., Pan, H., Wu, X..,Guan, R., "Synthesis and properties of epoxy resin containing flexible segments". *Adhesion*, 36(11), 2015, pp.44-47+43.
20. Derrick, M., "Fourier transform infrared spectral analysis of natural resins used in furniture finishes". *Journal of the American Institute for Conservation*, 28(1), 2013, pp.43-56.
21. Cholake, S. T., Mada, M. R., Raman, R.K. S., Bai, Y., Zhao, X., Rizkalla, S., Bandyopadhyay, S., "Quantitative analysis of curing mechanisms of epoxy resin by mid-and near-fourier transform infra red spectroscopy". *Defence Science Journal*, 64(3), 2014, pp.314-321.
22. Vashurkin, D. V., Malkov, G. V., Karpov, S. V., Garifullin, N. O., Kapasharov, A. T., "The method of the extent of epoxy-amine cure reaction determination by near infra-red spectroscopy". *Key Engineering Materials*, 5997(5997), 2019, pp.180-186.
23. Weiss, S., Seidl, R., Kessler, W., Kessler, R. W., Zikulnig-Rusch, E. M., Kandelbauer, A., "Multivariate curve resolution (MCR) of real-time infrared spectra for analyzing the curing behavior of solid MF thermosetting resin". *International Journal of Adhesion and Adhesives*, 110, 2021. pp.102956.
24. Kissinger, H. E., "Reaction kinetics in differential thermal analysis". *Analytical Chemistry*, 29(11), 2002, pp.1702-1706.
25. Crane, L. W., Dynes, P. J., Kaelble, D. H., "Analysis of curing kinetics in polymer composites". *Journal of Polymer Science: Polymer Letters Edition*, 11(8), 1973, pp.533-540.
26. Starink, M. J., "The determination of activation energy from linear heating rate experiments:a comparison of the accuracy of isoconversion methods". *Thermochimica Acta*, 404(1), 2003, pp.163-176.